Influence of different fibers on the change of pore pressure of self-consolidating concrete exposed to fire

Yining DING [1*], Cong ZHANG [1], Mingli CAO [2] and Yulin ZHANG [3], Cecília Azevedo [3]
[1]State Key Laboratory of Coastal and Offshore Engineering, Dalian University of Technology, Dalian 116000, China
[2] Institute of Building Materials, School of Civil Engineering, Dalian University of Technology, Dalian 116000, China
[3] Centre of Mathematics, University of Minho, Braga 4700-052, Portugal

Abstract: The focus of this paper is given to investigate the effect of different fibers on the pore pressure of fiber reinforced self-consolidating concrete under fire. The investigation on the pore pressure-time and temperature relationships at different depths of fiber reinforced self-consolidating concrete beams was carried out. The results indicated that micro PP fiber is more effective in mitigating the pore pressure than macro PP fiber and steel fiber. The composed use of steel fiber, micro PP fiber and macro PP fiber showed clear positive hybrid effect on the pore pressure reduction near the beam bottom subjected to fire. Compared to the effect of macro PP fiber with high dosages, the effect of micro PP fiber with low fiber contents on the pore pressure reduction is much stronger. The significant factor for reduction of pore pressure depends mainly on the number of PP fibers and not only on the fiber content. An empirical formula was proposed to predict the relative maximum pore pressure of fiber reinforced self-consolidating concrete exposed to fire by considering the moisture content, compressive strength and various fibers. The suggested model corresponds well with the experimental results of other research and tends to prove that the micro PP fiber can be the vital component for reduction in pore pressure, temperature as well spalling of concrete.

Key words: Pore pressure; Spalling; Fire; Fibers; Self-consolidating concrete; Hybrid effect

1. Introduction

Fire poses one of the most serious risks to concrete for underground construction and above ground structure because it often results in explosive spalling of concrete. Reinforcing bars directly exposed to fire due to concrete spalling will further aggravate the fire risk, since it is very likely to cause sudden failure of concrete structures during fire exposure [1-5]. Two main mechanisms can explain the fire spalling of concrete [6-9]. One is related to the thermo-mechanical process [6, 9], which is associated with the temperature field and the mismatch of thermal expansion between cement matrix and aggregate in concrete, as illustrated in Fig. 1a. The other one is related to the thermo-hydral process (pore pressure theory), which is directly related to the mass transfer of vapor, water and air in the porous network. This thermo-hydral process will result in building up high pore pressures and pressure gradients, as shown in Fig. 1b [9]. According to pore pressure theory, the vapour pressure will dramatically increase at the boundary between the vapour zone and humid zone (Fig. 1b). Around the peak of the vapour pressure, since high vapour pressure in concrete generates a large tensile stress, concrete spalling

would occur [10, 11].

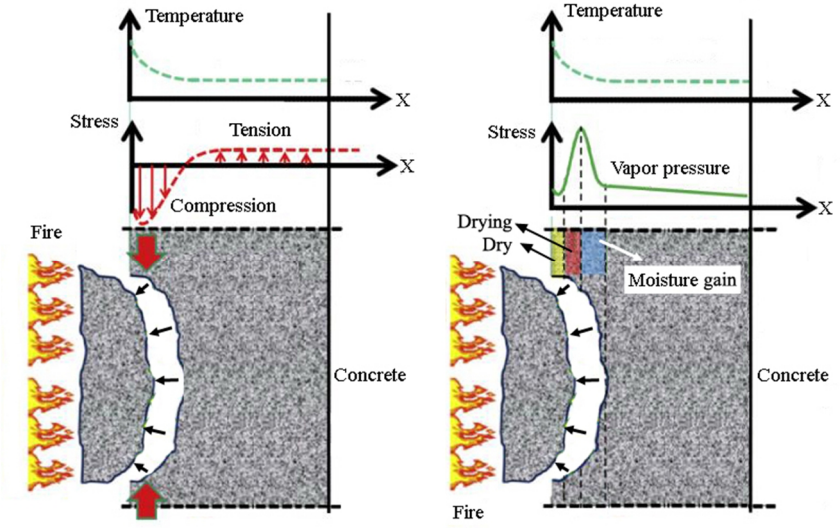

(**a**) (**b**)

Fig. 1 Mechanisms of concrete spalling (**a**) Thermal stress theory; (**b**) Pore pressure theory [9]

Quantitative analysis of pore pressure in concrete is one of the difficulties to investigate the fire spalling. The previous studies usually focus on the pore pressure development in ordinary concrete and high-strength concrete exposed to electric heating [12-16, 20]. However, the investigation on the pore pressure of concrete and fiber reinforced self-consolidating concrete (FRSCC/SCC) during fire exposure is very limited [17, 18], although SCC/ FRSCC are gaining considerable interest in concrete structures and underground constructions like shield tunnel segment.

This paper presents an experimental study of the fiber effect on the pore pressure in SCC during fire exposure. Steel fiber, micro polypropylene (PP) fiber, macro PP fiber and the composition were employed in this study. Influence of mono fiber and hybrid fibers on the pore pressure - time and temperature relationships of SCC were investigated. The effect of different mixes of fibers is presented in this paper. The study of pore pressure development leads to a better understanding of spalling in SCC and FRSCC during fire exposure.

2. Experiment

2.1 Materials

In this program, the mix design of FRSCC was as follows: Cement (P•O 52.5R), fly ash, fine sand, crushed stone were used. The amount of superplasticizer (Sika, polycarboxylic acid type, ASTM C494 type F, the highest water reduction is up to 30%) was 1.2 wt.% of binder content. The base mix design of SCC without fiber reinforcement is illustrated in Table 1.

Table 1 Mix proportion of plain SCC /(kg/m^3)

Materials	Cement	Fly ash	Water	Sand 0-5 mm	Crushed stone 5-15 mm	Superplasticizer	W/B ratio
Content	400	160	180	764.8	832	6.72	0.32

The investigated fibers can be divided into micro fibers (l < 3 cm) and macro fibers ($l \geq 3$

cm). The micro PP fibers are mainly used to decrease the shrinkage cracks and to prevent the spalling [3-5] at the high temperature. The steel fibers are used for increasing the flexural toughness and for restricting and bridging the macro cracks before heating and to enhance the residual behavior during and after the high temperature. Images and basic properties of fibers used in this study are shown in Fig. 2 and Table 2, respectively. The various fiber contents (kg/m^3), the air content and the compressive strengths of different mixtures before heating are summarized in Table 3 and Table 4.

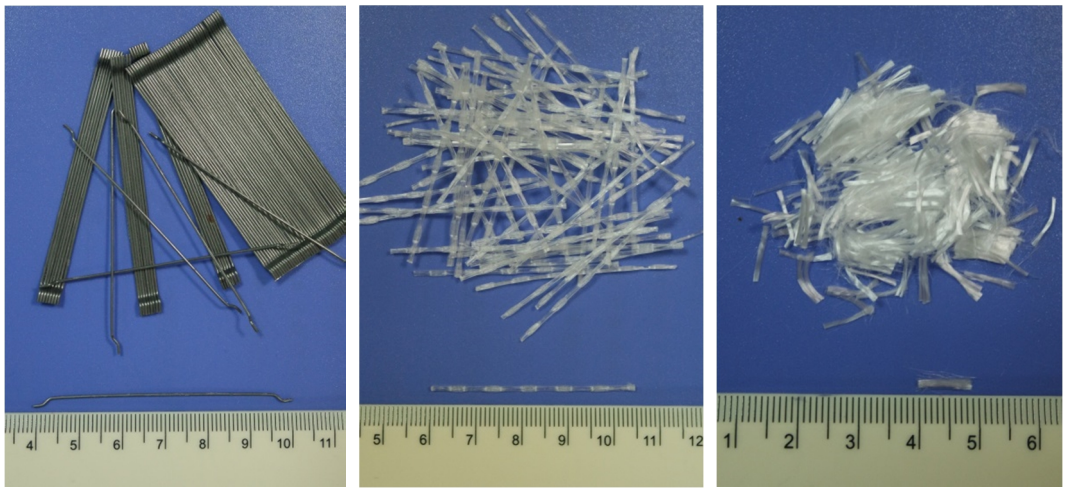

(**a**) (**b**) (**c**)

Fig. 2 Images of fibers used in this study (**a**) Steel fiber; (**b**) Macro PP fiber; (**c**) Micro PP fiber

Table 2 Properties of fibers

Materials	Density (g/cm^3)	Geometric size	Tensile strength (N/mm^2)	Quantity (pieces/kg)	Melting temperature (^{o}C)
Steel fiber	7.85	Hooked l_f = 60 mm d_f= 0.75 mm	≥1100	4600	—
Micro PP fiber	0.91	Straight l_f =9 mm d_f=18 μm	615	3.5 billion	170
Macro PP fiber	0.91	Double duoform l_f =45 mm d_f=0.74 mm	465	50140	170

Table 3 Dosage of different fiber combinations /(kg/m^3)

Groups / Fibers	1 PC	2 Micro PPF1	3 SF50	4 Macro PPF4	5 SF40+Micro PPF1	6 SF40+Macro PPF4	7 SF40+MicroPP F05+Macro PPF2
Micro PP fiber	0	1	0	0	1	0	0.5
Steel fiber	0	0	50	0	40	40	40
Macro PP fiber	0	0	0	4	0	4	2

Table 4 Air content, moisture content and compressive strength of different mixtures before heating

Groups	Air content /%	Moisture content /%	Compressive strength /MPa
1 PC	2.3	4.5	63.2
2 Micro PPF1	3.4	4.2	61.5
3 SF50	2.9	4.7	65.3
4 Macro PPF4	3.1	4.7	67.0
5 SF40+Micro PPF1	3.8	4.5	63.8
6 SF40+Macro PPF4	3.5	4.9	67.2
7 SF40+Micro PPF05+Macro PPF2	4.2	4.3	62.2

From Table 3 and Table 4, it can be seen that the air content of the fresh concrete increases with the increasing of fiber dosage. The compressive strength of all series was between 60 and 70 MPa. The moisture content of the concrete specimens was between 4 and 5% by mass. The specimens with a size of 150mm×150mm×550mm were employed for pore pressure tests. During the moulding of concrete, metal tubes were inserted. The end of the tube was placed at different pressure measurement points, i.e. depth of 10, 20 and 30 mm, as illustrated in Fig. 4a. After casting, all the specimens were stored in a standard curing room of concrete with molds for 24 hours. Thereafter they were demoulded, subjected to 20 ^{o}C water and cured for 28 days.

2.2 Fire test setup

As shown in Fig. 3, the pressure gauge [12, 13] was made of porous sintered metal net with evenly distributed pores of diameter 4 μm. A metal tube with inner diameter of 2 mm was connected with the metal cup. Prior to heating, the metal tube was filled with silicon oil having a fire point of 315 ^{o}C. The fire test set-up is demonstrated in Fig. 4a.

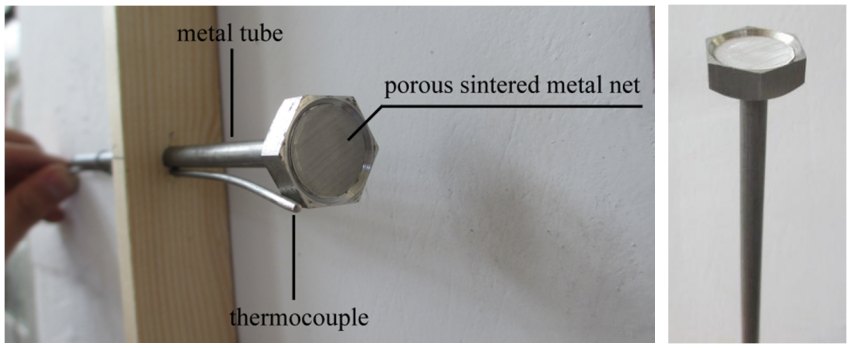

Fig. 3 Pressure gauge and thermocouple used in this study

The thermal load was applied on the bottom of the concrete beam, as shown in Fig. 4a. The burning experiment is carried out according to the temperature – time curve of ISO 834-1. The whole temperature-rising process of the beam is controlled by the gas temperature. In order to investigate the fire spalling and pore development of SCC, the specimen was exposed to the maximum temperature of 600 ^{o}C. As shown in Fig. 4b, the temperature of the gas increases up to 600^{o}C in 6 min, after that it remains stable for 120 min at 600 ^{o}C then falls down naturally to the room temperature.

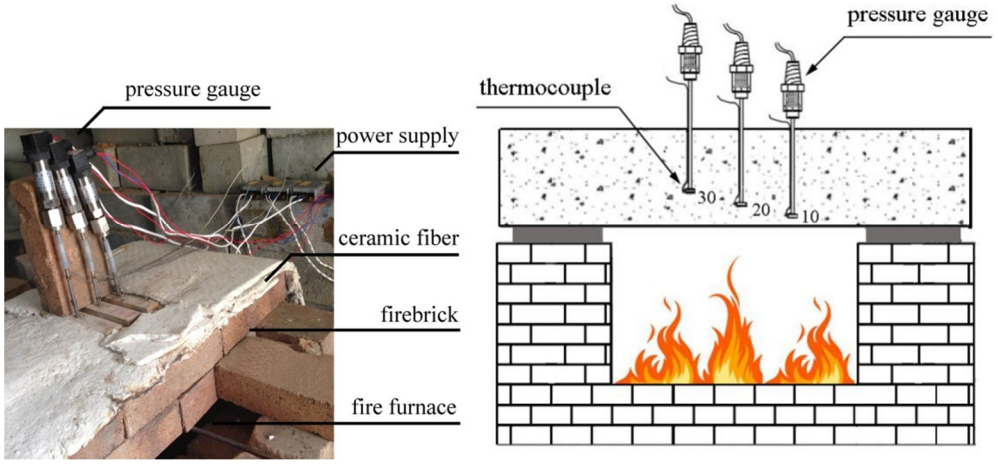

(**a**) (**b**)

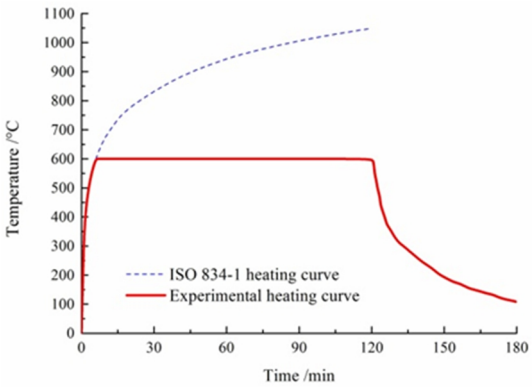

(**c**)

Fig. 4 (**a**) Fire test set-up; (**b**) Schematic diagram of pressure gauge at different depths of SCC beam and (**c**) Experimental T-t curve for pore pressure measurement

3. Results and discussion

3.1 Pore pressure development

The pore pressure development of plain SCC and FRSCC with various fibers during fire exposure will be analyzed in this section. The comparison of the pore pressure-time curves of beams with or without fibers in three measure points at different depth of 10 mm, 20 mm and 30 mm during fire exposure are illustrated in Fig. 5.

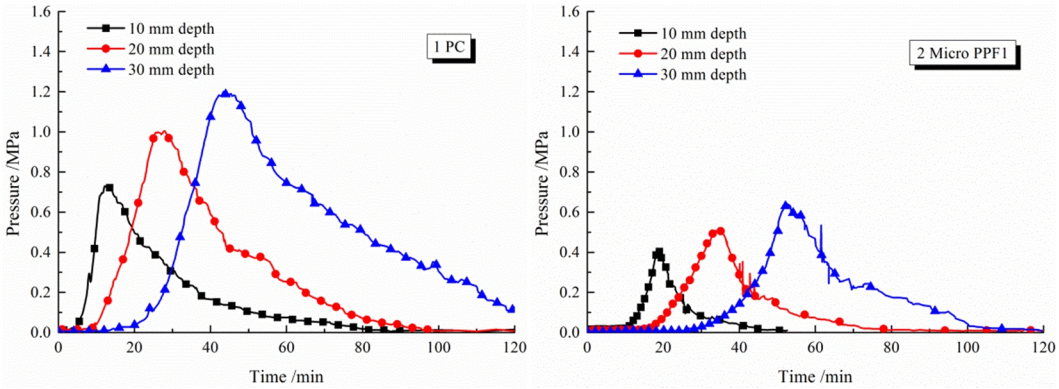

(**a**) (**b**)

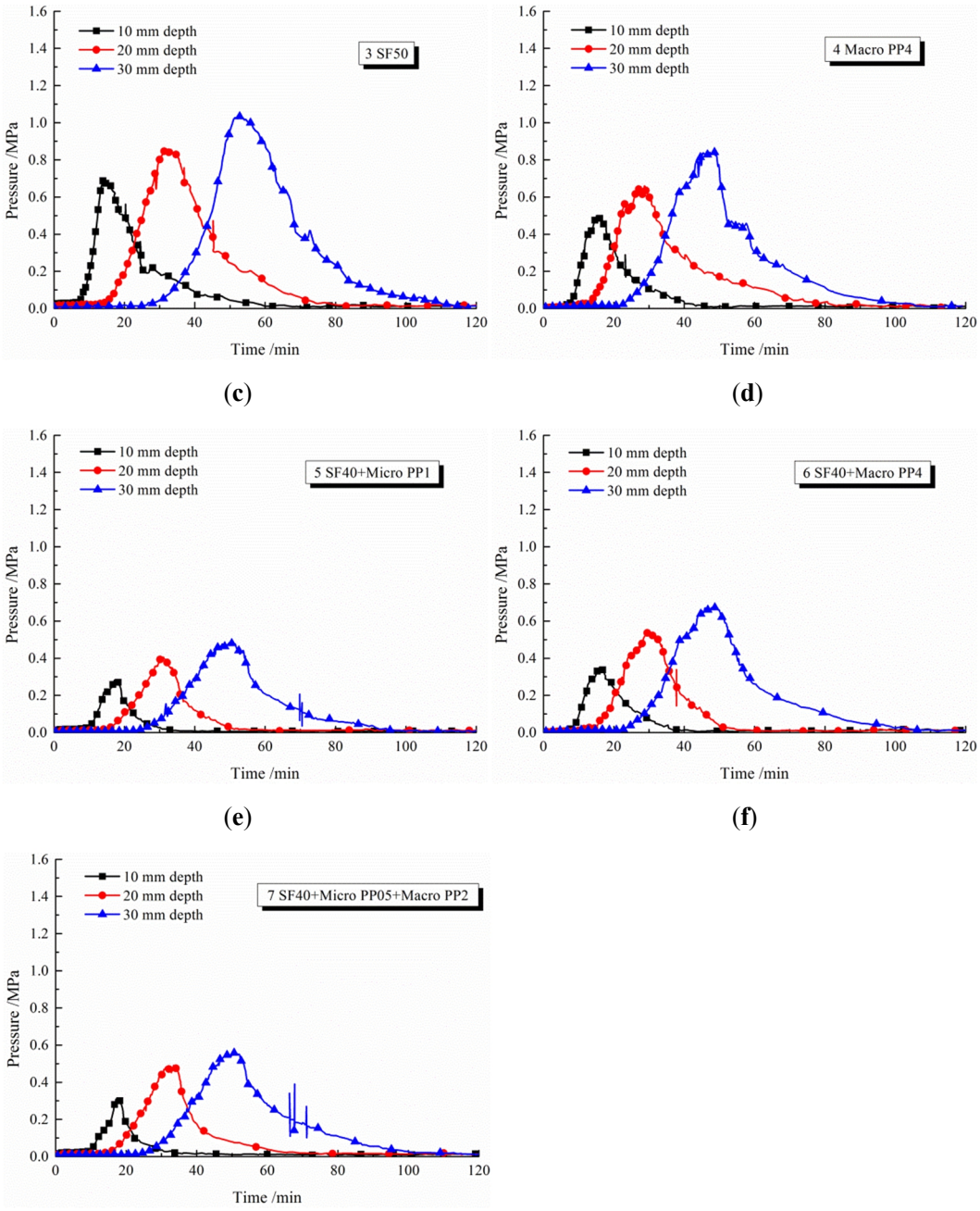

Fig. 5 Comparison of pore pressure-time curves of beams with or without fibers during fire exposure

In order to analyze the fiber effect on the pore pressure change, two new terms "pore pressure reduction P_R" and "the decreasing ratio of pore pressure D_R" are introduced and can be expressed in Eq.(1) and Eq.(2):

$$P_R = \Delta P = P_{SCC} - P_{FRSCC} \tag{1}$$

$$D_R = \frac{P_R}{P_{SCC}} \times 100\% = \frac{P_{SCC} - P_{FRSCC}}{P_{SCC}} \times 100\% \tag{2}$$

From Fig. 5, it can be seen that:

(1) The maximum pore pressures measured in plain SCC at all depths are much higher than those of FRSCC. The fibers were very effective in building up percolated system in concrete matrix [19]. Therefore, the pore pressure reduction in FRSCC is somewhat likely due to the introduction of percolated pathways after adding fibers into the un-percolated concrete. These pathways are very likely the percolation in the interfacial transition zones around fibers (Fig. 6), which can improve the evaporation and permeability of pore pressure of concrete under fire exposure.

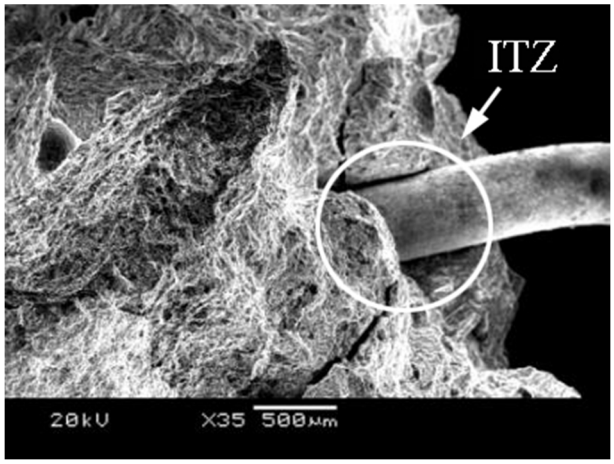

Fig. 6 ITZ between steel fiber and matrix after 600°C [3]

(2) The pore pressure at the depth of 30 mm of different beams shows the highest value of the three measure points. Compared to the pressure of the same beam at 20 and 30 mm, the value of pore pressure at the depth of 10 mm is the lowest. It may highlight the importance of permeability to the build-up of pore pressure of concrete under the high temperature.

(3) Compared to plain SCC, the descending branch of pore pressure-time curve of FRSCC drops more severely. This is likely due to the pore pressure reduction effect of fibers via the introduction of numerous pathways.

Table 5 shows the comparison of the peak pressure and its occurrence time in different depths of all tested samples. Table 6 presents the decreasing ratio of pore pressure and prolonged rate of the occurrence time of peak pressure in different depths.

Table 5 Comparison of peak pressure and the occurrence time in different depths

Samples	10 mm		20 mm		30 mm	
	Pressure /MPa	Time /min	Pressure /MPa	Time /min	Pressure /MPa	Time /min
1 PC	0.73	13.3	1.01	27.9	1.19	43.4
2 Micro PPF1	0.40	18.4	0.51	33.7	0.64	52.7
3 SF50	0.69	14.1	0.85	33.2	1.02	53.0
4 Macro PPF4	0.50	15.1	0.66	28.7	0.84	48.4
5 SF40+Micro PPF1	0.28	14.8	0.40	30.7	0.49	50.1
6 SF40+Macro PPF4	0.35	16.5	0.54	29.6	0.68	46.0

7 SF40+Micro PPF05+Macro PPF2	0.31	17.9	0.48	33.4	0.56	50.5

Table 6 Decreasing ratio of pore pressure and prolonged rate of the occurrence time of peak pressure in different depths

Samples	10 mm		20 mm		30 mm	
	Pressure /%	Time /%	Pressure /%	Time /%	Pressure /%	Time /%
1 Plain	0	0	0	0	0	0
2 Micro PP	45.2	38.3	49.5	20.8	46.2	21.4
3 SF	5.5	6.0	15.8	19.0	14.5	22.1
4 Macro PP	31.5	13.5	34.7	2.9	19.4	11.5
5 SF+Micro PP	61.6	11.3	60.4	10.0	58.8	15.4
6 SF +Macro PP	52.1	24.1	46.5	6.1	42.9	6.0
7 SF+MicroPP+Macro PP	57.5	34.6	52.5	19.7	53.0	16.3

From Table 5 and 6, it can be seen that:

(1) The addition of fibers can delay the occurrence time of the peak value of pore pressure in different depths, e.g., the peak value of pore pressure of plain SCC in the depth of 30 mm occurs at about 43.4 min, while the occurrence time of peak value of pore pressure of FRSCC ranges from 46 min to 53 min. This can be explained by the moisture clog theory [10, 11]. When a concrete specimen is heated, the pressure in the pores will rise near the surface. The pressure gradient then drives moisture towards the inner colder regions and the vapor will condense gradually, until a fully saturated region (moisture clog) is created. Further movement of vapor towards the colder regions will be restricted by this moisture clog, thus results in a rapid rise in pore pressure. The introduction of numerous ITZ around fibers enhances the permeability of FRSCC, which will inversely hinder the formation and development of moisture clog, thus delays the occurrence of maximum pore pressure.

(2) Compared to SCC without micro PP fibers, the FRSCC specimens containing micro PP fibers show lower pore pressure and longer time to reach peak value of pore pressure. Micro PP fiber plays a stronger role in reducing pore pressure than that of macro PP fiber and steel fiber at different depths of 10 mm, 20 mm and 30 mm. Compared to plain SCC, the addition of 1 kg/m^3 micro PP fiber brings 46.2% reduction to the maximum pore pressure, from 1.19 MPa to 0.64 MPa, while the mono use of 50 kg/m^3 steel fiber and 4 kg/m^3 macro PP fiber only brings 14.5% and 19.4% reduction, respectively. It means that the micro PP fibers can be more effective to reduce the pore pressure than macro PP fiber and steel fiber.

3.2 Influence of mono fiber on pore pressure development

Fig. 7 shows the comparison of relationships between pore pressure and temperature of plain SCC and mono fiber reinforced SCC. The comparisons of peak values of the pore pressure and corresponding temperature for mono fiber reinforced SCC Aare illustrated in Table 7.

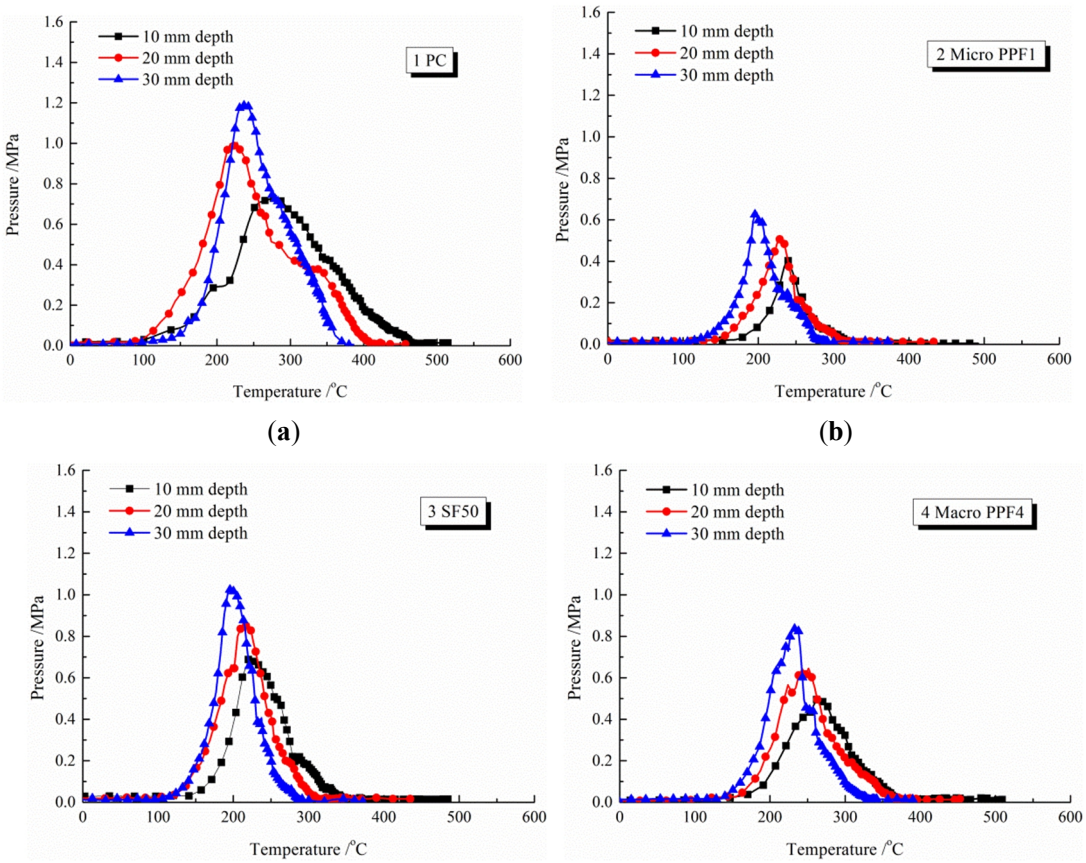

Fig. 7 Comparison of pore pressure - temperature relationships for plain SCC and mono fiber reinforced SCC.

Table 7 Comparison of temperature at peak pressure for mono fiber reinforced SCC /°C

Groups	Depth of 10 mm	Depth of 20 mm	Depth of 30 mm
1 PC	277	227	240
2 Micro PPF1	240	229	199
3 SF50	221	217	197
4 Macro PPF4	262	252	235

From Fig. 7 and Table 7, the following results can be drawn:

(1) The addition of SF shows some effect on the pore pressure reduction in deeper regions (i.e. 20 mm and 30 mm depth) of SCC exposed to fire (see Fig. 8). This observation is also confirmed by M. R. Bangi [14, 15]. Two reasons may account for this phenomenon. One of the reasons can be the creation of discrete bubbles during the mixing process, and the bubbles may act as a kind of discontinuous reservoirs for pressure relief [14]; and the another reason is that the relatively high pressure will increase the possibility of pressure relief via/at the interface of steel fiber [15].

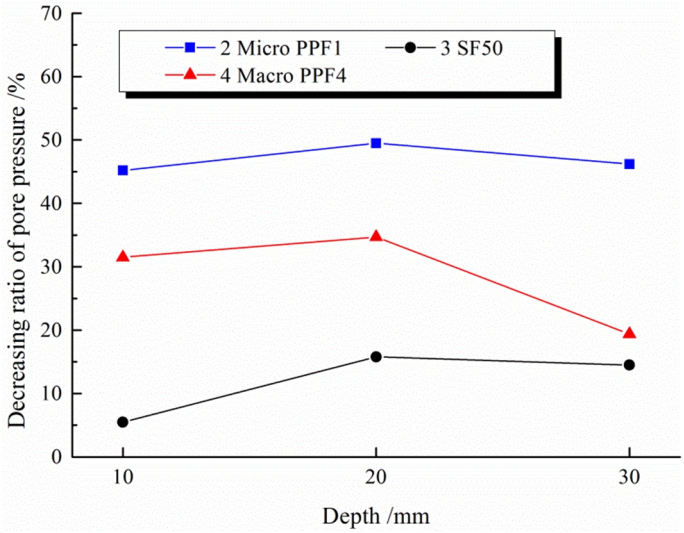

Fig. 8 Relationship between decreasing ratio of pore pressure and depth for mono fiber reinforced SCC

(2) The pore pressure can be reduced by using of macro PP fibers more effectively than by steel fibers. Meanwhile, Fig. 8 illustrates that the addition of macro PP fiber shows stronger effect in reduction of pore pressure near the bottom (e.g. in depth of 10 mm) than that in deep regions during fire exposure. Two of the important reasons can be as follows: a) macro PP fibers melt and vaporize due to the lower melting point (160 ^{o}C-180 ^{o}C), and b) after being melted and vaporized, large number of free spaces in the macro channels in the concrete matrix will create, which can release the pore pressure clearly during the heating process (see Fig. 9).

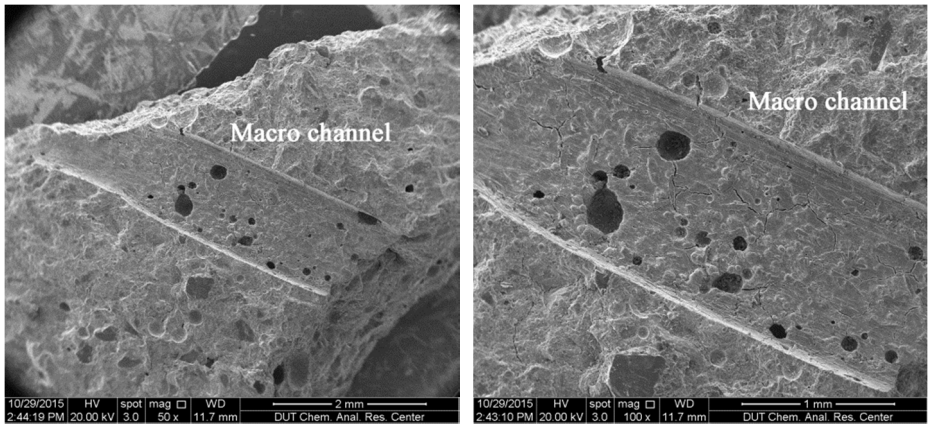

Fig. 9 SEM image of macro channel caused by macro PP fiber after 600 ^{o}C

(3) Micro PP fiber is more effective in mitigating maximum pore pressure development compared to macro PP fiber and steel fiber. For micro PP fiber or macro PP fiber reinforced SCC, the maximum pore pressure occurred in the temperature of 199 ^{o}C and 235 ^{o}C. It means that the pore pressure relief occurs after melting of PP fibers, since the melting temperature of PP fiber is around 160-180 ^{o}C.

3.3 Influence of hybrid fibers on pore pressure development

Fig. 10 shows the comparison of the relationship between the pore pressure and temperature

for hybrid FRSCC during fire exposure. Table 8 presents the comparison of the peak values of pore pressure and the corresponding temperature for hybrid fiber reinforced SCC.

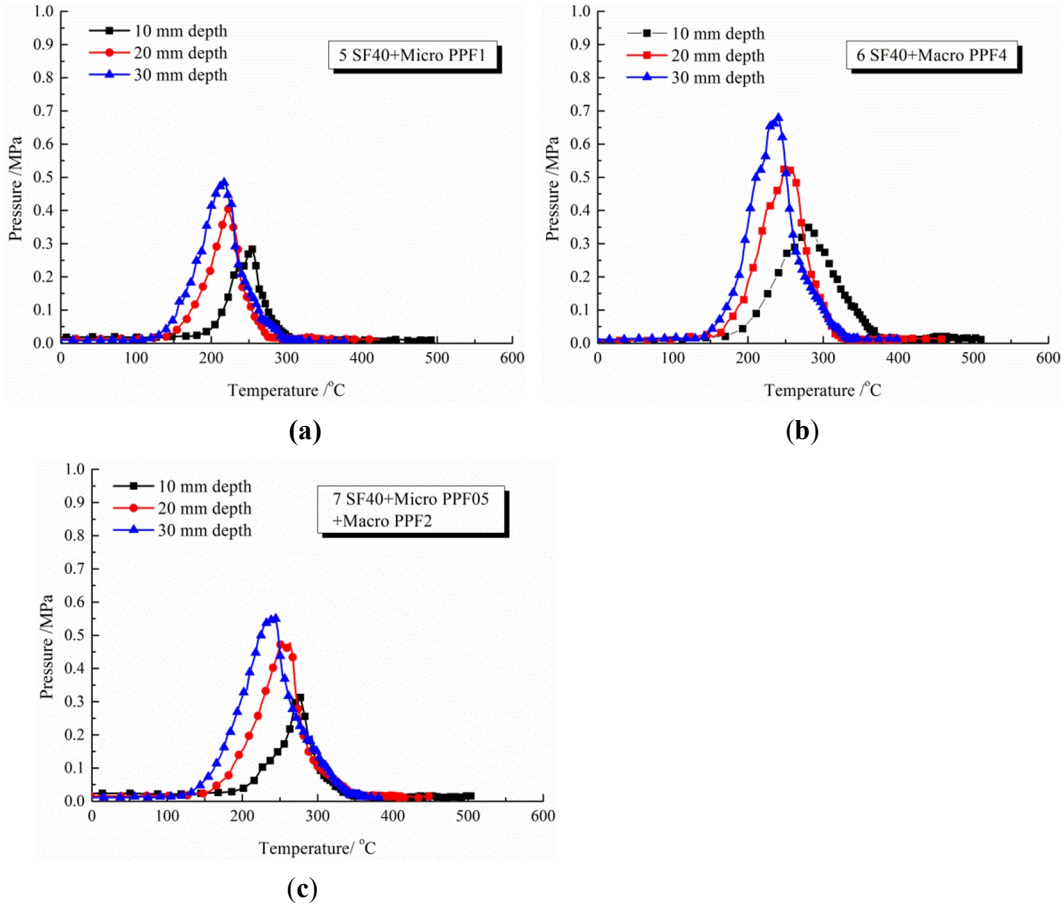

Fig. 10 Comparison of the Pore pressure – Temperature relationships of hybrid FRSCC

Table 8 Comparison of the peak pore pressure and the corresponding temperature for hybrid fiber reinforced SCC

Groups	Depth of 10 mm	Depth of 20 mm	Depth of 30 mm
5 SF40+Micro PPF1	255	222	210
6 SF40+Macro PPF4	280	250	240
7 SF40+Micro PPF05+Macro PPF2	270	263	242

From Fig. 10 and Table 8, it can be seen that:

(1) Compared to mono SF reinforced SCC, the hybrid fibers reduce the pore pressure at different depths of 10 mm, 20 mm and 30 mm, the diphasic use of SF40 and micro PPF1 shows stronger effect on the reduction of the pore pressure.

(2) The micro PP fibers show the strongest effect on reduction of the pore pressure of all the three fiber types. Two of the important reasons can be as follows [3]: a) PP fibers melt and vaporize due to the lower melting point (160 °C-180 °C), and b) the huge amount of micro PP fibers (3.5 billion/kg) are well distributed, melted and vaporized, making large number of free spaces in the micro-channels in the concrete matrix and releasing the pore pressure clearly during the heating process (see Fig. 11). In addition, micro PPF shows beneficial

effect on the residual strength of concrete after fire exposure, and decreasing tension stress in the capillary [3].

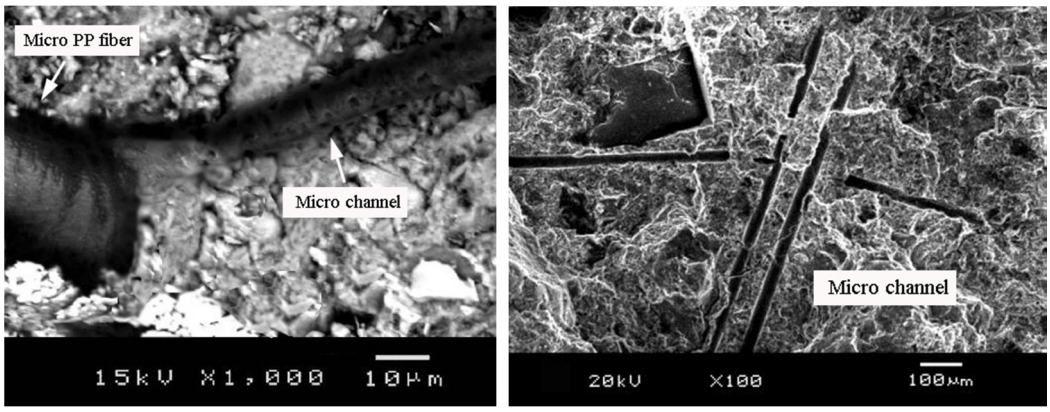

(**a**) (**b**)

Fig. 11 Image of micro PP fiber (**a**) After 200 ^{o}C [18] and (**b**) After 600 ^{o}C [3]

(3) The temperature at the corresponding peak value of pore pressures of diphasic fibers (SF40 and macro PPF4) and triphasic fibers (SF40+Micro PPF05+Macro PPF2) reinforced SCC is in the range between 240^{o}C and 280^{o}C, which is higher than that of SF40+Micro PPF1 reinforced SCC (210^{o}C -250^{o}C, see Table 8).

The discussion above indicates that the important influence factor on the decreasing of temperature may be due mainly to the increment of micro PPF content or pieces. Compared to micro PP fibers, the relative few number of macro PP fibers (50000 pieces/kg) with large geometric size in the matrix are unable to create so much free spaces for releasing of the pore pressure as those of micro PPF during the heating; and some few large free spaces due to melting of macro PPF are incapable to improve so strong diffusion and evaporation of heat and temperature as micro PPF. That means not all the PP fibers are capable to reduce the peak value of pore pressure, and the geometrical dimension of the PP fibers may play a remarkable role to affect the evaporation of pore pressure. The number of fibers per unit volume of micro PPF can be vital to reducing of both maximum pore pressure and temperature.

The influence of combined use of various fibers on the relationship between the decreasing ratio and the different measuring points along the beam depth is illustrated in Fig.12. It can be observed that compared to mono fiber reinforced SCC (Fig. 7), the hybrid use of fibers shows a relatively steady effect on the pressure reduction in all tested points (near the bottom at 10 mm and in the deep region at 20 mm and 30 mm).

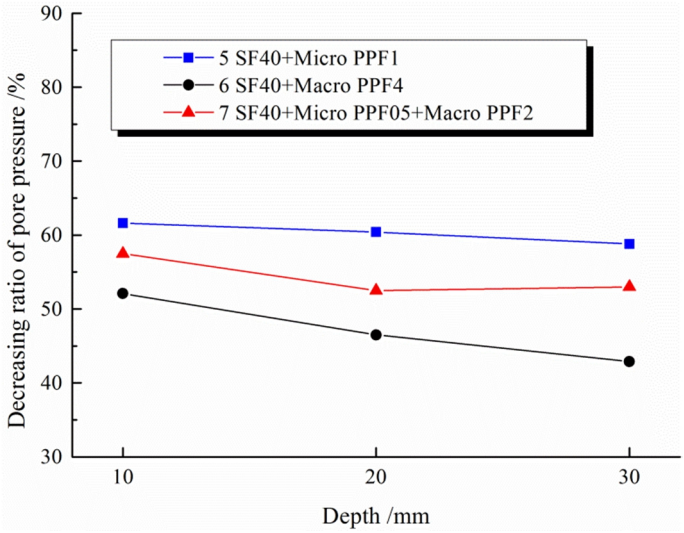

Fig. 12 Relationship between decreasing ratio of pore pressure and depth for hybrid fiber reinforced SCC

3.4 Hybrid effect of different fibers on pore pressure reduction

Fig. 13-15 shows the hybrid effect of different types of fiber in reducing pore pressure. The results are expressed as difference between pore pressure of FRSCC and the value of plain SCC on the y-axis versus the depth (mm) of the measure points on the x-axis in Fig. 13, Fig. 14 and Fig. 15. The comparison between hybrid effect of composed SF40+Micro PP1 and effect of the sum of mono SF40 and mono micro PPF1 on the pore pressure reduction P_R is plotted in Fig. 13.

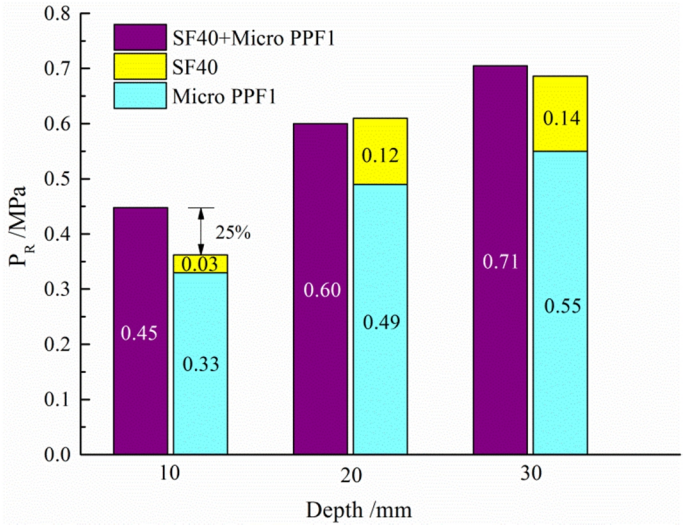

Fig. 13 Comparison between hybrid effect of composed SF40+Micro PPF1 and the effect of the sum of mono SF40 and mono micro PPF1 on P_R

It should be noted that:

(1) The values of P_R of SF40, micro PP1 and SF40+Micro PPF1 at the depth of 10 mm are 0.03, 0.33 and 0.45 MPa, respectively. Compared to the sum of mono macro SF40 and mono micro

PPF1, the pore pressure reduction of FRSCC specimen with composed SF40+Micro PPF1 is 25% higher.

(2) The values of P_R of SF40, micro PPF1 and SF40+Micro PPF1 at the depth of 20 mm are 0.12, 0.49 and 0.6 MPa, respectively. The value of specimen with composed SF40+Micro PPF1 is almost equivalent to that of the sum of specimen with mono macro SF40 and mono micro PPF1.

(3) The values of P_R of SF40, micro PP1 and SF40+PPF1 at the depth of 30 mm are 0.14, 0.55 and 0.71 MPa, respectively. Compared to the sum of specimen with mono macro SF40 and mono micro PPF1, the value of composed SF40+micro PPF1 increased slightly (only 2.9%).

(4) The diphasic use of macro SF40 and micro PPF1 shows a greater positive hybrid effect on P_R near the bottom at 10 mm than it achieved by the sum of mono fiber reinforced SCC in the deep regions at 20 and 30 mm.

The comparison between hybrid effect of diphasic use of SF40+Macro PPF4 and effect of the sum of mono macro SF40 and mono macro PPF4 on the pore pressure reduction P_R is illustrated in Fig. 14.

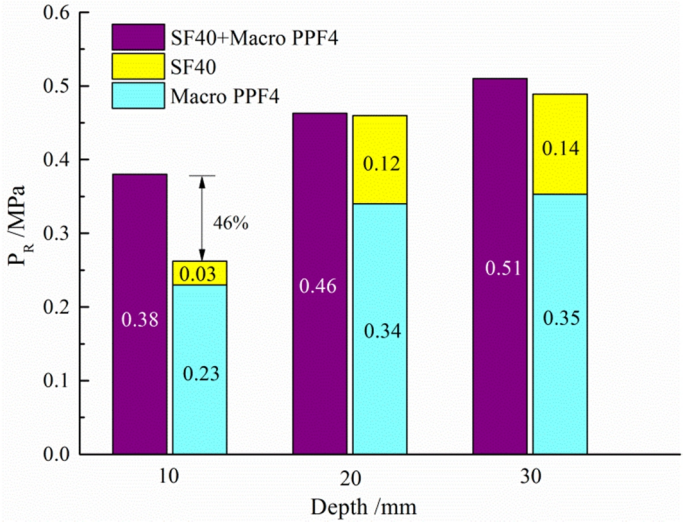

Fig. 14 Comparison between hybrid effect of composed SF40+Macro PPF4 and the effect of the sum of mono SF40 and mono macro PPF4 on P_R

From Fig. 14, it can be seen that:

(1) The values of P_R of SF40, macro PPF4 and SF40+Macro PPF4 at the depth of 10 mm are 0.03, 0.23 and 0.38 MPa, respectively. Compared to the sum of mono macro SF40 and mono macro PPF4, the value of specimen with composed SF40+Macro PPF4 is 46% higher.

(2) The values of P_R of SF40, macro PPF4 and SF40+Macro PPF4 at the depth of 20 mm are

0.12, 0.34 and 0.46 MPa, respectively. The value of specimen with diphasic use SF40+Macro PPF4 is almost equivalent to that of the sum with mono macro SF40 and mono macro PPF4.

(3) The values of P_R of SF40, macro PPF4 and SF40+Macro PPF4 at the depth of 30 mm are 0.14, 0.35 and 0.51 MPa, respectively. Compared to the sum of specimen with mono macro SF40 and mono macro PP4, the value of diphasic use of SF40+macro PPF4 increased slightly (only 4%).

(4) Similar to the phenomenon in Fig. 13, the discussion above indicates that the diphasic use of macro SF and macro PPF shows stronger positive hybrid effect on P_R near the bottom at 10 mm than that of the sum of mono fiber reinforced SCC in the deep regions at 20 and 30 mm.

(5) Compared to the effect of macro PPF4 in Fig.14, the effect of micro PPF1 (see Fig. 13) on P_R at 10mm, 20 mm and 30 mm increased 43.5%, 44.1% and 57.1% (see Fig.16a), respectively.

The comparison between hybrid effect of triphasic use of SF40+Macro PPF2+Micro PPF05 and effect of the sum of mono SF40, mono macro PPF2 and mono micro PPF05 on P_R is illustrated in Fig. 15.

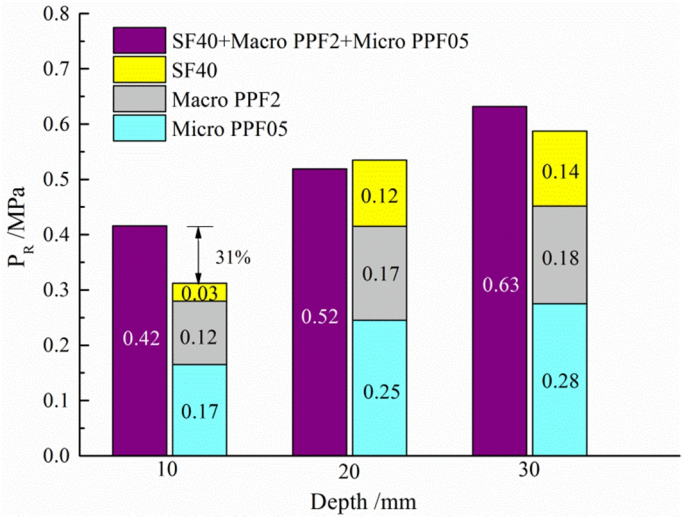

Fig. 15 Comparison between hybrid effect of composed SF40+Macro PPF2+Micro PPF05 and the effect of the sum of mono SF40, mono macro PPF4 and mono micro PPF05on P_R

From Fig. 15, it can be seen that:

(1) The values of P_R of SF40, macro PPF2, micro PPF05 and SF40+Macro PPF2+Micro PPF05 at the depth of 10 mm are 0.03, 0.12, 0.17 and 0.42 MPa, respectively. Compared to the sum of mono macro SF40, mono macro PPF2 and mono micro PPF05, the value of specimen with triphasic use of SF40+Macro PP2+Micro PPF05 is 31% higher.

(2) The values of P_R of SF40, macro PPF2, micro PPF05 and SF40+Macro PPF2+Micro

PPF05 at the depth of 20 mm are 0.12, 0.17, 0.25 and 0.52 MPa, respectively. The value of triphasic use of SF40+Macro PPF2+Micro PPF05 is very close to that of the sum with mono macro SF40, mono macro PPF2 and mono micro PPF05.

(3) The values of P_R of SF40, macro PPF2, micro PPF05 and SF40+Macro PPF2+Micro PPF05 at the depth of 30 cm are 0.14, 0.18, 0.28 and 0.63 MPa, respectively. Compared to the sum of mono SF40, mono macro PPF2 and mono micro PPF05, the value of triphasic use of SF40+Macro PPF2+Micro PPF05 increased about 5%.

(4) Similar to the phenomenon in Fig. 13 and Fig.14, the composed use of macro SF, micro PPF and macro PPF shows strong positive hybrid effect on pore pressure reduction near the bottom at 10 mm than it achieved by the sum of mono fiber reinforced SCC in the deep regions at 20 and 30 mm.

(5) Compared to the effect of macro PPF2, the effect of micro PPF05 on P_R at 10mm, 20 mm and 30 mm increased 41.7%, 47.0% and 55.6% (see Fig.16b), respectively.

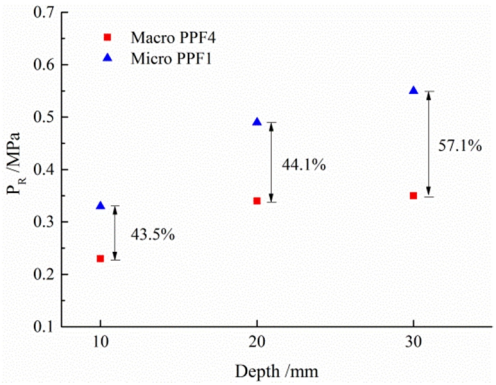

Fig. 16a Comparison of the effect on P_R between micro PPF1 and macro PPF4

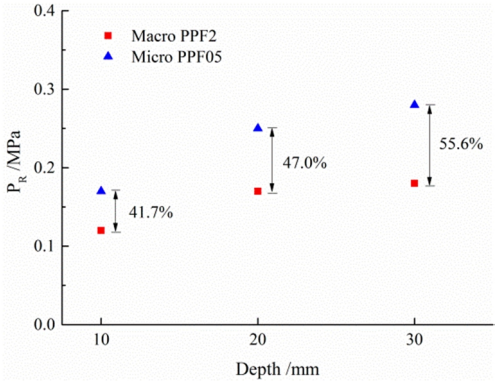

Fig. 16b Comparison of the effect on P_R between micro PPF0.5 and macro PPF2

From Fig. 13-16, it can be concluded that:

- The significant positive hybrid effect is found at 10 mm near the backfire surface of beam bottom.
- At the depth of 20 mm, the value of specimen with diphasic or triphasic use of SF+ macro/micro PP fiber is very close to the value of the sum with mono macro SF, mono macro PPF and mono micro PPF.
- Compared to the sum of specimen with mono SF, mono macro PPF and micro PPF at the depth of 30 cm, the value of diphasic or triphasic use of SF+macro/micro PPF increased slightly (between 2.8% and 5%).
- Compared to the effect of macro PPF4 in Fig.14, the effect of micro PPF1 (see Fig. 13) on P_R at 10mm, 20 mm and 30 mm increased 43.5%, 44.1% and 57.1% (see Fig.16a), respectively. Compared to the effect of macro PPF2, the effect of micro PPF05 on P_R at

10mm, 20 mm and 30 mm increased 41.7%, 47.0% and 55.6% (see Fig.16b), respectively. That means the significant factor for reducing of pore pressure depends mainly on the number of PP fibers or the cumulative surface area of total PP fibers and not only on the fiber content.

3.5 Observation of spalling of SCC and FRSCC

Spalling is the violent or non-violent breaking off of layers or pieces of concrete from the surface of a structural element when it is exposed to high and rapidly rising temperatures as experienced in fires [21, 22]. Spalling could be grouped into six categories: aggregate spalling, explosive spalling, surface spalling, sloughing off spalling, corner spalling and post cooling spalling [21]. The first three normally occur early into a fire while the last three normally occur later in a fire. Explosive spalling and surface spalling are violent, while sloughing off spalling is non-violent [22]. In this study, no violent spalling was found, but numerous micro cracks, as shown in Fig. 17. These observations were found in the case of plain SCC and all FRSCC. However, after 4 days all the tested beams present a severe but shallow flaking of concrete cover, as illustrated in Figure 18. It implies numerous micro cracks had been developed in SCC and FRSCC beams during the fire exposure.

(**a**) (**b**)

Fig. 17 Beam bottom surface after fire exposure: (**a**) Overall view showing no explosive spalling; (**b**) Magnified view of (a) showing numerous micro cracks. These observations were found in the case of plain SCC and all FRSCC

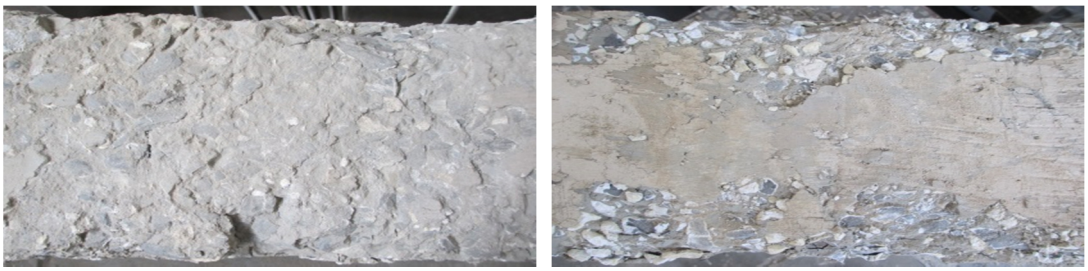

(**a**) SCC without fibers (**b**) SCC with SF50

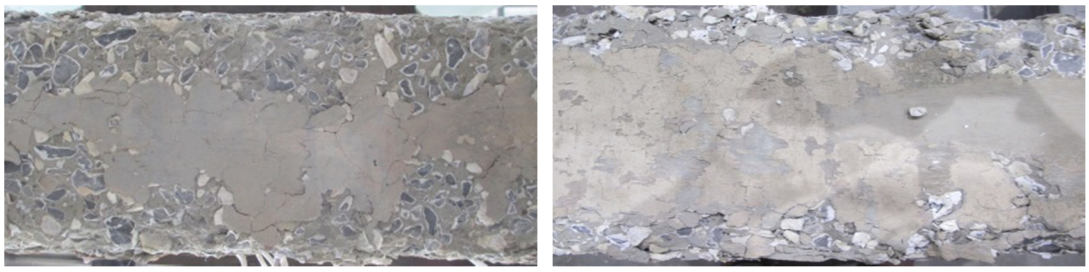

(**c**) SCC with SF40+Micro PPF1 (**d**) SCC with SF40+Macro PPF4

Fig. 18 Beam bottom surface after fire exposure of 4 days showing a severe but shallow flaking of concrete cover

From Fig. 18, it can be seen that the SCC beam without fibers suffers a more severe spalling than FRSCC, followed by SCC with SF50. From the perspective of pore pressure theory, when the pore pressure in concrete exceeds the tensile strength of the concrete under heating, spalling will occur. However, we can't make sure if the cracking and sloughing off behavior in Fig. 17 and Fig. 18 are totally caused by pore pressure directly, since the maximum pore pressure value measured in this study is lower than the tensile strength of SCC and FRSCC under heating, as shown in Fig. 19. Previous study points out in a single fire several of the six types of spalling could occur, even all of them [21, 22]. Therefore, the observations of spalling in this paper may not just relate to the pore pressure. Anyhow, further research is still needed.

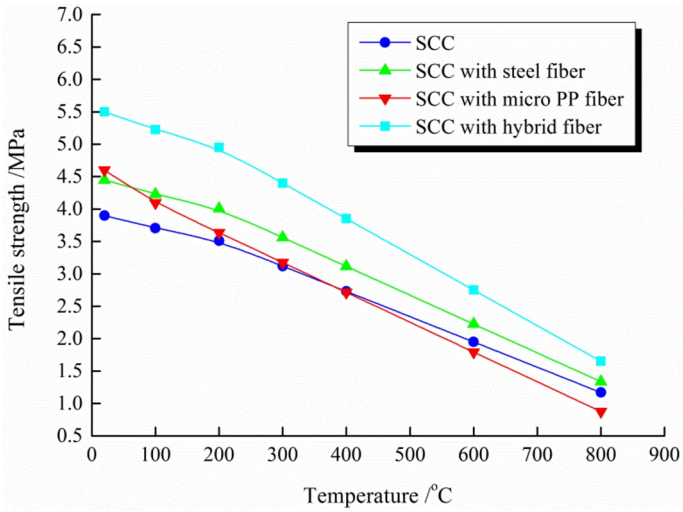

Fig. 19 Tensile strength (splitting tensile test) of SCC and FRSCC at different temperatures given by Kodur [23]

3.6 Prediction formula for the relative maximum pore pressures

In order to evaluate and to predict the relative maximum pore pressure $RMPP$, an empirical formula was proposed based on the regression analysis of the results of pore pressure development in FRSCC above mentioned, as shown in Eq. (3). The value of $RMPP$ is derived from dividing maximum pore pressure of FRSCC by the maximum pore pressure in plain SCC. The parameters considered in this empirical formula are the moisture content, compressive strength, the cumulative surface area of steel fiber, macro PP fiber and micro PP fiber. In general, low strength

concrete is superior to good concrete in spalling. Higher strength is usually achieved by reducing the water/binder ratio or adding fine mineral admixtures, which produce a dense concrete of very low permeability, thus enhancing pore pressure spalling (via lower permeability) but reduce thermal stress spalling (via higher strength). Therefore, the compressive strength of concrete before heating is one of the most important parameters for spalling prediction. Moisture content is another important parameter to understand pore pressure spalling. Moisture in concrete is the direct source of pore pressure at elevated temperatures. Previous studies indicated that explosive spalling may be eliminated when the moisture content of concrete is lower than 2.5%, however, concrete will suffer a high spalling risk when the moisture content is beyond 2.5%. The moisture content of the concrete specimens in this study is between 4 and 5% by mass. Therefore, the moisture content of concrete before heating should be another important parameter for spalling prediction. The formula of the predicted relative maximum pore pressure $PRMPP$ is expressed as Eq. (3). The comparison of relationships of $PRMPP$ and measured relative maximum pore pressure $MRMPP$ between plain SCC without fibers and FRSCC is shown in Fig. 20.

$$PRMPP = 0.298M + 0.003f_c - 0.005A_{sf} - 0.0025A_{micro\ pp} - 0.018A_{macro\ pp} \quad (3)$$

where $PRMPP$ is the predicted value of relative maximum pore pressure $RMPP$, M is the moisture content (%), f_c is the compressive strength of concrete before heating (MPa), A_{sf} is the cumulative surface area of steel fiber (m^2), $A_{micro\ pp}$ is the cumulative surface area of micro PP fiber (m^2) and $A_{macro\ pp}$ is the cumulative surface area of macro PP fiber (m^2).

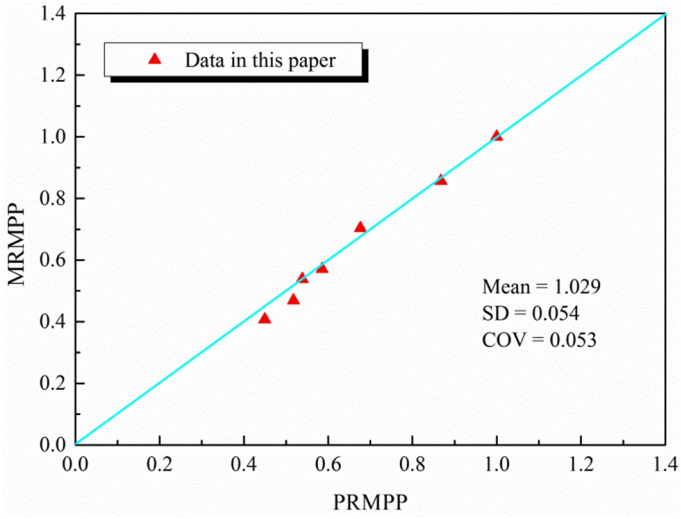

Fig. 20 Relationship between $MRMPP$ and $PRMPP$ in this study

It should be noted that Bangi MR [15] also presented a similar empirical formula in his paper. However, compared to Bangi's formula [15], the major difference in this work is the consideration of moisture content, thus making the modified prediction has a better agreement with experimental results.

In order to extend the validity of the proposed method for the relative maximum pore pressure, the prediction was modified including results in previous studies [14, 15, 17], as shown

in Table 9 and Fig. 21, which demonstrated the comparison of relationships of $PRMPP$ and $MRMPP$ between plain SCC without fibers and FRSCC. By comparing the $MRMPP$ and $PRMPP$ in Table 9 and Fig. 30, it can be seen that the predicted values based on the proposed model correlate well with the experimental results of fiber reinforced SCC samples, having a mean of 0.994, a standard deviation of 0.112 and a coefficient of variation of 0.112. Hence, if the parameters of moisture content, compressive strength and fiber conditions (content, type, size) are given, it is possible to predict the maximum pore pressure in SCC or HPC with different fiber-reinforcement exposed to fire. This prediction result can be an important reference during the design and optimization of mix proportion of the concrete used in the situation which may suffer a potential fire disaster.

Table 9 Results of $MRMPP$ and $PRMPP$ in previous studies

Data in paper [15]		Data in this paper		Data in paper [12, 13]	
PRMPP	MRMPP	PRMPP	MRMPP	PRMPP	MRMPP
1.00	1.04	1.00	1.01	0.10	0.15
0.79	0.79	0.54	0.54	0.18	0.17
0.69	0.68	0.87	0.86	0.22	0.26
1.06	0.96	0.68	0.70	0.22	0.21
0.87	0.84	0.45	0.41	0.29	0.23
0.74	0.73	0.59	0.57	0.30	0.28
		0.52	0.47	0.30	0.31
				0.37	0.44
				0.37	0.40
				0.48	0.49
				0.48	0.54
				0.50	0.60
				1.02	0.99

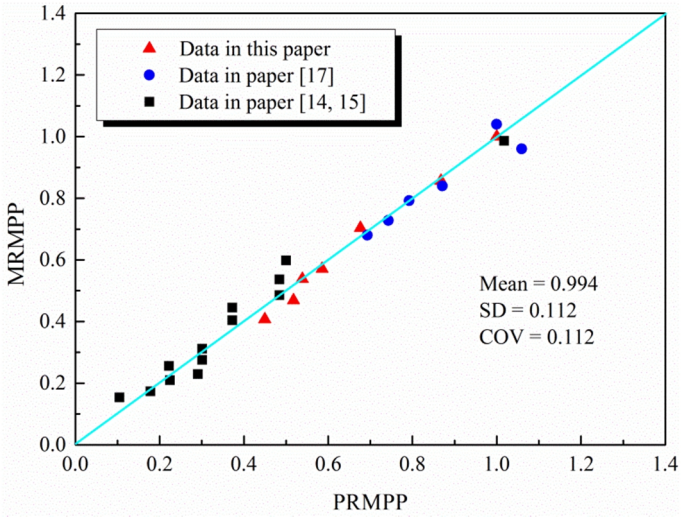

Fig. 21 Relationship between $MRMPP$ and $PRMPP$ in previous studies

4. Conclusions

From the experimental and analytical investigations above, the following conclusions may be drawn:

- The addition of fibers can delay the occurrence time of the peak value of pore pressure in different depths.
- The micro PP fibers show the strongest effect on the reduction of pore pressure of all the three fiber types. The fiber pieces per unit volume of micro PPF is vital to reducing of both maximum pore pressure and temperature.
- The addition of steel fiber plays some roles in pore pressure reduction in deeper regions of SCC exposed to fire. The inclusion of macro PP fiber plays a more efficient role in pore pressure reduction than steel fiber. Meanwhile, it seems that the addition of macro PP fiber has a better effect in shallow regions than in deep regions during fire exposure.
- Compared to the sum of mono fiber, the composed use (both diphasic use and triphasic use) of SF, micro PPF and macro PPF indicates clear positive hybrid effect on the pore pressure reduction on the bottom surface near flaming.
- Compared to the composed use of SF40+Macro PPF4 and SF40+Macro PPF2+Micro PPF05, the use of SF40+Micro PPF1 shows the strongest effect on the reduction of pore pressure in all different depths.
- Compared to the effect of macro PP fiber with high dosages, the effect of micro PP fiber with low fiber contents on the pore pressure reduction at various beam depth is much stronger. The significant factor for reduction of pore pressure depends mainly on the number of PP fibers and not only on the fiber content.
- An empirical model was suggested to predict the relative maximum pore pressure of FRSCC under fire. The results from predicted model agree well with tested values obtained by authors and other researchers. It means that the suggested model can be used to evaluate the relative maximum pore pressure of FRSCC.

Notation:

PC: Concrete specimen without fibers

SF: Steel fiber

PPF: Polypropylene fiber

SCC: Self-consolidating concrete

FRSCC: fiber reinforced self-consolidating concrete

SF40: Steel fiber reinforced SCC with fiber dosage of 40 kg/m^3

Micro PPF1: micro PP fiber reinforced SCC with fiber dosage of 1 kg/m^3

Macro PPF4: macro PP fiber reinforced SCC with fiber dosage of 4 kg/m^3

SF40+Macro PPF4: fiber cocktail reinforced SCC with 40 kg/m^3 macro steel fiber and 4 kg/m^3 macro PP-fiber

SF40+Micro PPF1: fiber cocktail reinforced SCC with 40 kg/m^3 macro steel fiber and 1 kg/m^3 micro PP fiber

SF40+Macro PP2+Micro PPF05: fiber cocktail reinforced SCC with 40 kg/m^3 macro steel fiber, 2 kg/m^3 macro PP fiber and 0.5 kg/m^3 micro PP fiber

HPC: high-performance-concrete

P_R: pore pressure reduction
D_R: decreasing ratio of pore pressure
PRMPP: predicted relative maximum pore pressure
MRMPP: measured relative maximum pore pressure

Acknowledgements
The authors acknowledge the National Natural Science Foundation of China (Grant: 51578109), the National Natural Science Foundation of China (Grant: 51121005), DUT and Fundaçãopara a Ciência e a Tecnologia (SFRH/BPD/22680/2005), the FEDER Funds through "Programa Operacional Factores de Competitividade - COMPETE" and by Portuguese Funds through FCT-within the Projects PEst-CMAT/UI0013/2011 and PTDC/MAT/112273/2009.

References
[1] Heo Y, Han C, Kim K. Combined fiber technique for spalling protection of concrete column, slab and beam in fire. Materials and Structures 2015, 48: 3377-3390.
[2] Ding Y, Wang Y, Zhang Y, et al. Investigation of the Stress and Strain State of Clay Pipes Under Fire Condition. Ceramics International 2009, 35: 63-67.
[3] Ding Y, Azevedo C, Aguiar J, et al. Study on Residual Behaviour and Flexural Toughness of Fiber Cocktail Reinforced Self Compacting High Performance Concrete after Exposure to High Temperature. Construction & Building Materials 2012, 26(1): 21-31.
[4] Dugenci O, Haktanir T, Altun F. Experimental research for the effect of high temperature on the mechanical properties of steel fiber-reinforced concrete. Construction and Building Materials 2015, 75: 82-88.
[5] Ma Q, Guo R, Zhao Z, et al. Mechanical properties of concrete at high temperature-A review. Construction and Building Materials 2015, 93: 371-383.
[6] Toropovs N, Monte F, Wyrzykowski M, et al. Real-time measurements of temperature, pressure and moisture profiles in high-performance concrete exposed to high temperature during neutron radiography imaging. Cement and Concrete Research 2015, 68: 166-173.
[7] Liu X, Ye G, Schutter GD. On the mechanism of polypropylene fibers in preventing fire spalling in self-compacting and high-performance cement paste. Cement and Concrete Research 2008, 38: 487-499.
[8] Ye G, Liu X, Schutter GD. Phase distribution and microstructural changes of self-compacting cement paste at elevated temperature. Cement and Concrete Research 2007, 37: 978-987.
[9] Mitsuo O, Shinya U, Toshiro K. Study of mechanisms of explosive spalling in high-strength concrete at high temperatures using acoustic emission. Construction and Building Materials 2012, 37: 621-628.
[10] Anderberg Y. Spalling phenomena in HPC and OC. In: Phan LT, Carino NJ, Duthinh D, Garboczi E, editors. Proceedings of the international workshop on fire performance of high-strength concrete. Gaithersburg, MD: NIST; 1997, 69–73.
[11] Khoury GA, Majorana FP, Schrefler BA. Modelling of heated concrete. Mag. Concr Res 2002; 54: 77-101.
[12] Kalifa P, Chene G, Christophe G. High-temperature behavior of HPC with polypropylene fibers: From spalling to microstructure. Cement and Concrete Research 2001, 31: 1487-1499.
[13] Kalifa P, Menneteau FD, Quenard D. Spalling and pore pressure in HPC at high temperatures.

Cement and Concrete Research 2000, 30: 1915-1927.
[14] Bangi MR, Horiguchi T. Pore pressure development in hybrid fiber-reinforced high strength concrete at elevated temperatures. Cement and Concrete Research 2011, 41: 1150-1156.
[15] Bangi MR, Horiguchi T. Effect of fiber type and geometry on maximum pore pressures in fiber-reinforced high strength concrete at elevated temperatures. Cement and Concrete Research 2012, 42: 459-466.
[16] Mindeguia JC, Pimienta P, Noumowe A, et al. Temperature, pore pressure and mass variation of concrete subjected to high temperature - Experimental and numerical discussion on spalling risk. Cement and Concrete Research 2010, 40: 477-487.
[17] Ye G, Schutter GD, Taerwe L. Spalling behavior of small self-compacting concrete slabs under standard fire conditions. 5th International RILEM Symposium on Self-Compacting Concrete, 3-5 September 2007, Ghent, Belgium.
[18] Jansson R, Bostrom L. The influence of pressure in the pore system on fire spalling of concrete. Fire Technology 2010, 46: 217-230.
[19] Benze DP. Fibers, percolation, and spalling of high performance concrete. ACI Materails Journal 2000, 97: 351-359.
[20] Phan LT. Pore pressure and explosive spalling in concrete. Material Structures 2008, 41: 1623-1632.
[21] Khoury GA. Researching explosive spalling. Tunnels & Tunnelling International 2006, June 6: 41-45.
[22] Khoury GA. Spalling. Internal report, Imperial College, London, 2006. Chapter to be published in Book on “Effect of heat on concrete, 2008”, Khoury GA and Majorana CE.
[23] Wasim K, Kodur V. Thermal and mechanical properties of fiber reinforced high performance self-consolidating concrete at elevated temperatures. Cement and Concrete Research 2011, 41: 1112-1122.